Analysis of streamflow response to land use land cover changes using satellite data and hydrological modelling: case study of Dinder and Rahad tributaries of the Blue Nile (Ethiopia/Sudan)

Khalid Hassaballah[1, 2, 3], Yasir Mohamed[1, 2, 3], Stefan Uhlenbrook[1, 2, 4], Khalid Biro[3]

[1]UNESCO-IHE Institute for Water Education, P.O. Box 3015, 2601DA Delft, The Netherlands

[2]Delft University of Technology, P.O. Box 5048, 2600 GA Delft, The Netherlands

[3]The Hydraulics Research Center, P.O. Box 318, Wad Medani, Sudan

[4]Unesco Italia, UN World Water Assessment Programme

Correspondence to: Khalid Hassaballah (k.hassaballah@yahoo.com)

Abstract. Understanding the land use and land cover changes (LULCC) and its implication on surface hydrology of the Dinder and Rahad basins (D&R) approximately 77,504 km^2 is vital for the management and utilization of water resources in the basins. Although there are many studies on LULCC in the Blue Nile basin, specific studies on LULCC in the D&R are still missing. Hence, its impact on streamflow is unknown. The objective of this paper is to understand the LULCC in the Dinder and Rahad and its implications on streamflow response using satellite data and hydrological modelling. The hydrological model has been derived by different sets of LULC maps from 1972, 1986, 1998 and 2011. Catchment topography, land cover and soil maps, are derived from satellite images and serve to estimate model parameters. Results of LULCC detection between 1972 and 2011 indicate a significant decrease of woodland and an increase of cropland. Woodland decreased from 42% to 14% and from 35% to 14% for Dinder and Rahad respectively. Cropland increased from 14% to 47% and from 18% to 68% in Dinder and Rahad respectively. The model results indicate that streamflow is affected by LULCC in both the Dinder and the Rahad Rivers. The effect of LULCC on streamflow is significant during 1986 and 2011. This could be attributed to the severe drought during mid 1980s and the recent large expansion in cropland.

Keywords: land use land cover, PCRaster, hydrological modelling, streamflow response, WFlow model, Dinder Rahad

1   Introduction

Streamflow is an important hydrological variable needed for water resources planning and management, and for ecosystem conservations. The rainfall runoff process over the upper Dinder and Rahad basins (D&R) is complex, non-linear, and exhibits temporal and spatial variability. To manage water resources effectively at a local level, decision makers need to understand

5   how human activities and climate change may impact local streamflow. However, the impact is often not well understood with locally obtained data such as observed flow. For this reason, we used satellite data and hydrological modelling to analyze the land use and land cover changes (LULCC) and its impacts on streamflow response in the D&R.

The D&R generate around 7% of the Blue Nile basin's annual flow. The Rahad River supplies water to the Rahad Irrigation Scheme (100,000 ha), while the Dinder River supplies water to the diverse ecosystem of the Dinder National Park

10   (DNP). The DNP (10,291 km^2) is a vital ecological area in the arid and semi-arid Sudan-Saharan region.

The Dinder and Rahad Rivers ~~has~~ experienced significant changes in floodplain hydrology during recent years, claimed to be caused by land use land cover changes in the upstream catchment. The floodplain hydrology defines the seasonal wetlands (Mayas) which are the only source of water in the DNP during the dry season (8 months). The hydrology of the mayas has large implications on the ecosystem of the DNP. A detailed description of the mayas wetlands can be found in ~~(Hassaballah~~ et

15   al., 2016).

LULCC was identified as a key research priority with multi-directional impacts on both human and natural systems (Turner II et al. 2007). Many studies highlighted the impacts of LULCC on hydrology (DeFries and Eshleman 2004; Uhlenbrook 2007), on ecosystem services (DeFries and Bounoua 2004; Metzger et al. 2006; Polasky et al. 2011) and on biodiversity (Hansen et al. 2004; Hemmavanh et al. 2010).

20   LULCC is a widespread observable phenomenon in the Ethiopian highlands as pointed by (Zeleke and Hurni 2001; Bewket and Sterk 2005; Hurni et al. 2005; Teferi et al. 2013;). These studies have pointed out different types and rates of LULCC in different parts of the Ethiopian highlands over different time periods and reported that the expansion of croplands associated with a decrease in woodlands have been the general forms of transitions.

Recently, Gumindoga et al. (2014) assessed the effect of land cover changes on streamflow in the Upper Gilgel Abbay

25   river basin in northwestern Ethiopia. Their results showed significant land cover changes where cropland has changed from 30% of the catchment in 1973 to 40% in 1986 and 62% in 2001. The study attributed these changes to the increase in population, which increased the demands for agricultural land. The study has also pointed that farmers in the area are commonly clearing forests to create croplands, and the resulting effect was the decrease in forest land from 52% in 1973 to 33% in 1986 and 17% in 2001. Since the Upper Blue Nile basin is neighboring the D&R, one may expect some similarities of

30   catchment characteristics, though differences cannot be excluded. These transitions have contributed to the high rate of soil erosion and land degradation in the Ethiopian plateau (Bewket and Teferi 2009). Understanding the impacts of LULCC on hydrology, and incorporating this understanding into the emerging focus on LULCC science are the most important needs for the future (Turner et al. 2003).

Many models have been developed to simulate impacts of LULCC on streamflow. These can be categorized as an

35   empirical black box, conceptual, and physically based distributed models. Each type of these three models has its own advantages and limitations. Several situations in practice demand the use of simple tools such as the linear system models or black box models. Nevertheless, these simpler models usually fail to mimic the non-linear dynamics, which are essential in the rainfall-runoff transformation process. Therefore, the development of a dynamic modelling language within a GIS framework such as PCRaster is a further important stage that allows complex models, like the WFlow rainfall-runoff model,

40   to be implemented making use of globally available spatial data sets. The PCRaster programming language is an environmental modelling language to build dynamic spatial environmental models (Bates and De Roo 2000; Karssenberg 2002; Uhlenbrook et al. 2004). Such spatially distributed models also have the potential to help in answering questions of policymakers about the impact of spatial changes (e.g. impacts of LULCC on streamflow dynamic). It has been shown that a variety of probable

LULCC impacts on hydrologic processes in the D&R are likely to happen. Therefore, the objective of this study is to understand the LULCC in the D&R and its impacts on streamflow response using satellite data, GIS and remote sensing, and hydrological modelling. The WFlow distributed hydrological model (Schellekens, 2011) is used simulate the processes. In addition, understanding the level to which the streamflow has altered is critical for developing an effective management plan

5   for ecosystem restoration and conservation. Thus, the Indicators of Hydrological Alteration (IHA) approach proposed by Richter et al. (1996), was then applied to analyze the streamflow characteristics likely to effect the ecological processes in the D&R including: flow magnitude, timing, and rate of change of flow.

2   Study area

The Dinder and the Rahad are the lower sub-basins of the Blue Nile River basin located between longitude 33°30' E and 37°30'

10   E and latitude 11°00' N and 15°00' N (Fig. 1). The Blue Nile basin collects flows of eight major tributaries in Ethiopia besides the two main tributaries in Sudan: the Dinder and the Rahad Rivers. Both tributaries derive their water from the runoff of the Ethiopian highlands approximately 30 km west of Lake Tana (Hurst et al. 1959). ~~Their~~ catchment areas are about 34,964 and 42,540 km^2 for the Dinder and the Rahad, respectively, giving a total area of about 77,504 km^2. The catchment has varied topography with elevation ranges between about 384 m at the catchment outlet and up to 2731 m at the Ethiopian plateau. The

15   D&R have a complex hydrology, with varying climate, topography, soil, vegetation and geology (Hassaballh et al. 2016). The annual average flow is about 2.797 x 10^9 and 1.102 x 10^9 m^3/year for the Dinder and the Rahad, respectively.
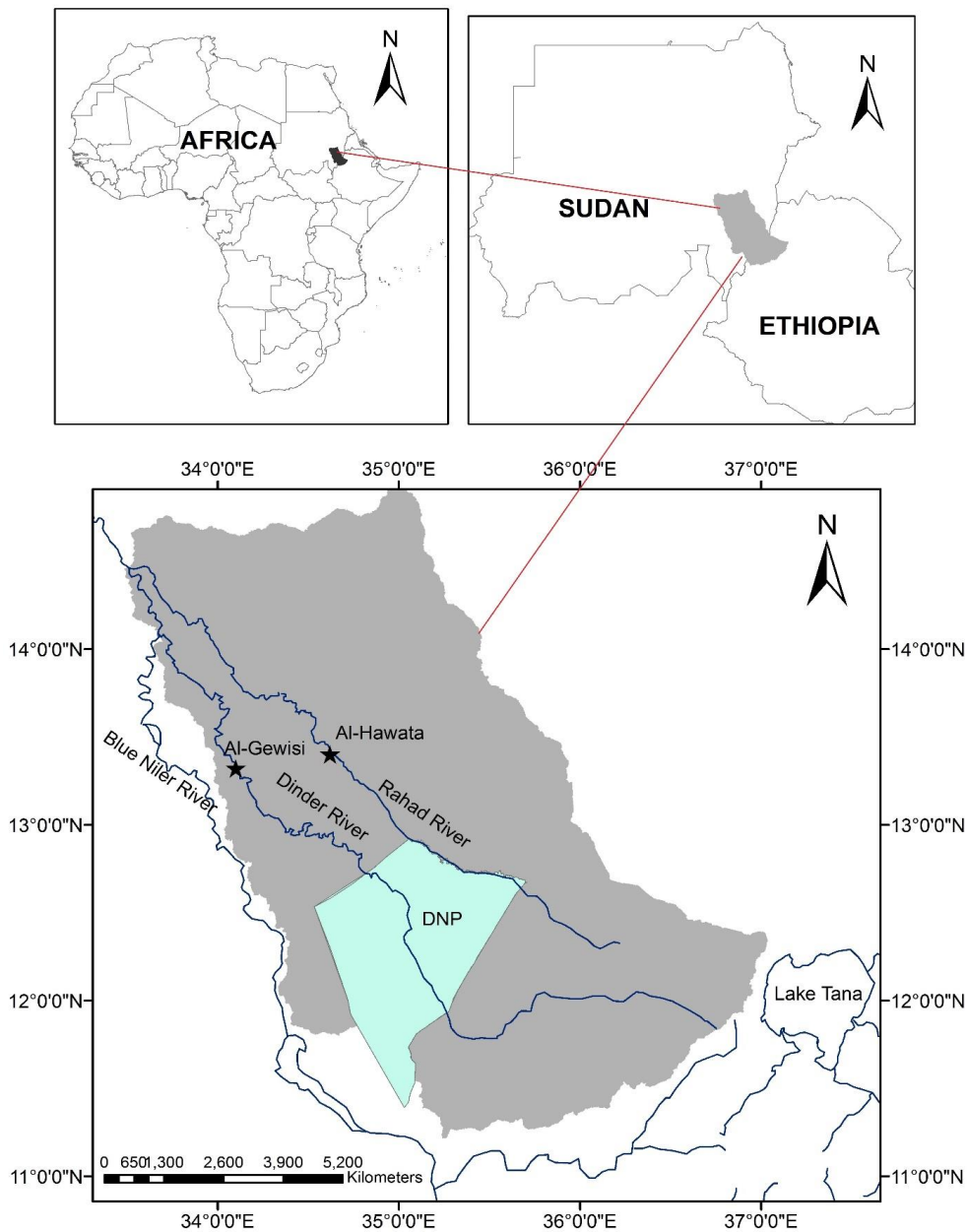
Figure 1. Location map of the Dinder and Rahad basins and the DNP. The two black stars are the hydrological stations (Al-Gewisi and Al-Hawata).

3   Data and Methods

5   Limited data is available for simulating the hydrology of the D&R. To fill this data gap, use has been made of globally available free datasets. The datasets which have been used to run the WFlow model are divided into two datasets; static data and dynamic data.

3.1   Input data

3.1.1   Static data

The static data contain maps that do not change over time. It includes maps of the catchment delineation, Digital Elevation Map (DEM), gauging points, land use, local drainage direction (*ldd*), outlets and rivers. These maps were created with a pre-prepare processes of the WFlow hydrologic model.

The catchment boundary has been delineated based on a 90 m x 90 m digital elevation map (DEM) of the NASA Shuttle Radar Topographic Mission (SRTM) obtained from the Consortium for Spatial Information (CGIAR_CSI) website (http://srtm.csi.cgiar.org).

Multi-temporal Landsat data for the years 1972, 1986, 1998 and 2011 were obtained free of charge from the internet site of the United States Geological Survey (USGS) (source: http://glovis.usgs.gov/). All images were geometrically corrected into the Universal Transverse Mercator (UTM) coordinate system (Zone-36N).

The soil map was obtained free of charge from the Food and Agriculture Organization (FAO) Harmonized World Soil Database (HWSD). The original catchment boundary layer provided 44 Soil Mapping Units (SMU) classes. These classes have been reclassified into 8 dominant soil group (DSG) categories, based on the DSG of each soil mapping unit code. These categories are: vertisols 71%, luvisols 9%, nitisols 8%, leptosols 5%, cambisols 4%, alisols 2% and fluvisols 1%. The map was then projected to WGS-84-UTM -zone-36N and resampled to a horizontal resolution of 500 m.

3.1.2   Satellite based rainfall and evapotranspiration data

The dynamic data contain maps that change over time. It includes daily maps of the precipitation and evapotranspiration. These maps were created with a pre-prepare step1 and step2 of WFlow model. In this study, three open-access satellite-based rainfall estimates (SBRE) products were compared based on their runoff performance at Al-Gewisi and Al-Hawata stations the outlets of the Dinder and Rahad basins, respectively. The best product was then used to run the WFlow model using different LULC maps. The SBRE and the evapotranspiration products used in this study are: Rainfall Estimates (RFE 2.0), potential evapotranspiration (PET), Tropical Rainfall Measuring Mission (TRMM) and Climate Hazards Group InfraRed Precipitation with Stations (CHIRPS).

The RFE 2.0 and the PET data were obtained from the Famine Early Warning System Network (FEWS NET). The horizontal resolution is 0.1 degree (11.0 km) for the RFE and 1.0 degree (110 km) for PET. This data is available on a daily basis from 2001 to near real-time period of record. More description can be found at http://earlywarning.usgs.gov/adds/downloads/.

The TRMM is a joint space mission between NASA and the Japan Aerospace Exploration Agency (JAXA) launched in 1997. TRMM product uses a multi-satellite precipitation analysis (TMPA), which includes also ground measurements provided by the Global Precipitation Climatology Center (GPCC). The TRMM has a spatial resolution of 0.25° and a temporal resolution of 3 hours. More information can be found in Huffman and Bolvin (2013), and on www.trmm.gsfc.nasa.gov.

The CHIRPS data were developed by the Climate Hazards Group (CHG) and scientists at the U.S. Geological Survey Earth Resources Observation and Science Center. This product is a new quasi-global precipitation with daily to seasonal time scales, a 0.05° resolution, and 1981 to near real-time period of record. The CHIRPS uses the monthly Climate Hazards Precipitation Climatology (CHPClim), the InfraRed (IR) sensors from the Group on Earth Observations (GEO) satellites, the TRMM 3B42 product, and the ground precipitation observations. More information about TRMM data can be found in Funk et al. (2014). A summary of all precipitation and evapotranspiration satellite products was provided in Table 1.

Hydrology and
Earth System
Sciences
Discussions

Table 1: Summary of the different precipitation and evapotranspiration satellite products

Product	Developer	Spatial resolution	Covering area	Temporal resolution	Time span	Ground measurement
TRMM v7	NASA, JAXA	0.25°	0°E-360°E/50°N-50°S	3 hourly	Jan 1998 - present	Yes
RFE 2.0	NOAA (CPC)	0.1°	20°E-55°E/40°N-40°S	6 Hourly	Jan 2001 - present	Yes
CHIRPS v2.0	CHG	0.05°	0°E-360°E/50°N-50°S	Pentads (Daily for Africa)	Jan 1983 - present	Yes
PET	NOAA (CPC)	1.0°	20°E-55°E/40°N-40°S	6 Hourly	Jan 2001 - present	Yes

3.1.3 Observed hydrological streamflow

Daily streamflow data at Al-Gewisi station on the Dinder River and at Al-Hawata station on the Rahad River for the period (2001-2012) were obtained from the Ministry of Water Resources, Irrigation and Electricity-Sudan. This data is mainly used for calibration and validation of the WFlow hydrological model.

3.2 LULC classification and change detection

LULC images were selected in the same season to minimize the influence of seasonal variations on the classification result. In order to cover all the study area, more than one scene of the satellite data was obtained, and consequently all images were mosaicked. The classification results of the historical images 1972, 1986 and 1998 were validated through visual interpretation of the unclassified satellite images and supported by in-depth interview of local elders. The classification of the 2011 image was validated by ground survey during a field visits throughout the study area during the period between 2011 and 2013 assuming no significant change during this period. A Global Positioning System (GPS) device was used to obtain exact location point data for each LULC class included in the classification scheme and for the creation of training sites and for signature generations as well. Moreover, field notes, site descriptions, and terrestrial photographs were taken to relate the site location to scene features. A total of (120) training areas were selected based on image interpretation keys, established during the field survey and from interviews with the local people. This later step was used as a crosscheck validation for the visual interpretation performed to the historical images. A supervised Maximum Likelihood Classification (MLC) technique was independently employed to the individual images. MLC is the most common supervised classification method used with remote sensing image data (Ellis et al. 2010; Pradhan and Suleiman 2009). The derivation of MLC is generally acceptable for remote sensing applications and is used widely (Richards et al. 2006).

The accuracy assessment of the classified images was based on the visual interpretation of the unclassified satellite images (Biro et al. 2013). However, the visual interpretation was conducted by an independent analyst not involved in the classification. The stratified random sampling design, where the number of points was stratified to the LULC types, was adopted in order to reduce bias (Mundia and Aniya 2006). Accordingly, error matrices as cross-tabulations of the classified data vs. the reference data were used to evaluate the classification accuracy. The overall accuracy, the user's and producer's accuracies, and the Kappa statistic values were then derived from the error matrices.

Multi-date Post-classification Comparison (PCC) change detection method described by Yuan et al. (2005) was used to determine the LULCC in three intervals: 1972–1986, 1986–1998 and 1998–2011. PCC is a quantitative technique that involves an independent classification of separate images from different dates for the same geographic location, followed by

a comparison of the corresponding pixels (thematic labels) in order to identify and quantify areas of change (Al Fugara et al. 2009; Jensen 2004). It is the most commonly used method of LULCC detection mapping (Kamusoko and Aniya 2009).

3.3 Description of the WFlow hydrological Model

In order to assess the impacts of LULCC on the streamflow dynamic, the WFlow distributed hydrological model (Schellekens, 2011) is forced using SBRE. The WFlow is a state-of-the-art open source distributed catchment model. The model is part of the Deltares OpenStreams project *(http://www.openstreams.nl)*. The model is derived from the CQFLOW model (Kohler et al., 2006). It is a hydrological model platform that includes two models: the WFlow_sbm model described by Verstessy and Elsenbeer (1999) derived from the TIOPG_SBM soil concept, and the WFlow_hbv model (distributed version of the HBV model). The model directly appeals to the need within the hydrological and geomorphologic sciences community to effectively use spatial datasets e.g. digital elevation models, land use maps, dynamic satellite data for rapid and adequate modelling of river basins with limited data availability. The model is programmed in PCRaster GIS dynamic language (Deursen 1995).

In this study, the WFlow_sbm PCRaster-based distributed hydrological model which makes use of the Gash and the TOPOG_SBM models was used. The model requires less calibration and maximizes the use of available spatial data that makes it a suitable model for this study. Step one of WFlow model was to delineate river network and the gauging points based on the DEM. Next, a land use and soil maps were added to the model and parameters were estimated based on physical characteristics of the soil and land use type. The rainfall interception was calculated using the Gash model (Gash 1979, 1995), while hydrologic processes that cause a runoff or overland flow were calculated using the TOPOG_SBM model. The WFlow uses potential evapotranspiration as an input data and derives the actual evaporation based on soil water content and vegetation cover type. The analytical Gash sub-model of rainfall interception in the WFlow is based on Rutter's numerical model. The surface runoff is modelled using a kinematic wave routine.

The model is fully distributed, which means that it makes the calculations for every grid cell of the basin. Each cell (500 m x 500 m) is seen as a bucket with a total depth divided to saturated and unsaturated stores (Fig. 2). The streamflow model results were then analyzed using the IHA approach described by Richter et al. (1996).
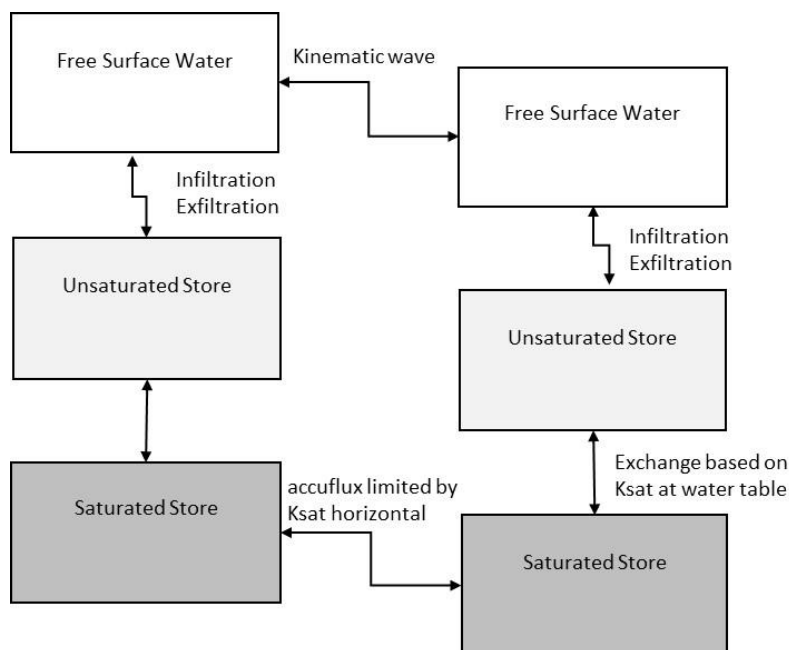
Figure 2. Schematization of the soil within the WFlow_sbm model

Source: http://WFlow.readthedocs.io/en/latest/WFlow_sbm.html#the-soil-model

5

3.3.1 Model calibration and validation

As with all hydrological models, calibration of the Dinder and Rahad hydrological model is needed for optimal performance. Since the hydrological data available for calibration start from 2001, the nearest land use (land use of 1998) was used in the calibration. The calibration procedure performed in two steps based on; firstly, initial values of all parameters were estimated

10 based on the land use and the soil types. Secondly, by adjusting the model parameters and evaluate the results.

The performance of the model was assessed using measures of goodness of fit between the modeled and observed flow using the coefficient of determination (R^2) and the Nash–Sutcliffe efficiency (NSE), defined by Nash and Sutcliffe (1970). The observed and the simulated flow of the Dinder and Rahad correlated well, except for few under-predictions and over-predictions of peak flows which can be explained in terms of inherent uncertainty in the model and the data. However, measures

15 of performances for both calibration and verification runs fell within the acceptable ranges.

3.4 Indicators of hydrologic alterations (IHA)

The IHA approach was introduced by Richter et al. (1996). The approach used to assess river ecosystem management objectives defined based on a statistical representation of the most ecologically relevant hydrologic indicators. These indicators describe the essential characteristics of a river flow that have ecological implications. A detailed description of IHA can be

20 found in (Richter et al., 1996 and Poff et al., 1997).

4   Results and Discussion

4.1   LULC classification and change detection

The overall LULC classification accuracy levels for the four images ranged from 82% to 87%, with Kappa indices of agreement ranging from 77% to 83% (Table 2). This accuracy is satisfactory for the study area considering the multi-temporal analysis of Landsat data and the visual interpretation adapted to image classification.

Table 2: Accuracy assessment (%) of LULC maps.

LULC Classes	1972		1986		1998		2011	
	Producer's	User's	Producer's	User's	Producer's	User's	Producer's	User's
Woodland	88	89	89	90	89	90	91	93
Cropland	78	70	80	74	80	80	83	82
Shrubland	71	71	73	75	77	75	80	75
Grassland	80	88	83	88	85	88	86	89
Bare Land	82	76	82	78	82	78	82	85
Water	86	86	88	86	91	86	94	86
Overall	82		84		85		87	
Kappa	77		79		81		83	

Landsat image classification results for the years 1972, 1986, 1998 and 2011 are shown in Fig. 3. According to the produced LULC maps, it was found that woodland, shrubland and grassland were the dominant types of LULC classes for the years 1972, while for the year 1986 they were shrubland, grassland and cropland. The LULC map of 1998 illustrates that the predominant types of LULC classes were cropland and woodland, while they were cropland and shrubs in 2011.

LULCC in the D&R are assessed by image comparison. In general, the results showed that the dominant process is the large decrease of woodland and increase of cropland. This result was in agreement with that of Rientjes et al. (1979) and Gumindoga et al. (2014), who studied the changes in land cover, rainfall and streamflow in the neighboring catchment of the upper Gilgel Abbay in Ethiopia.
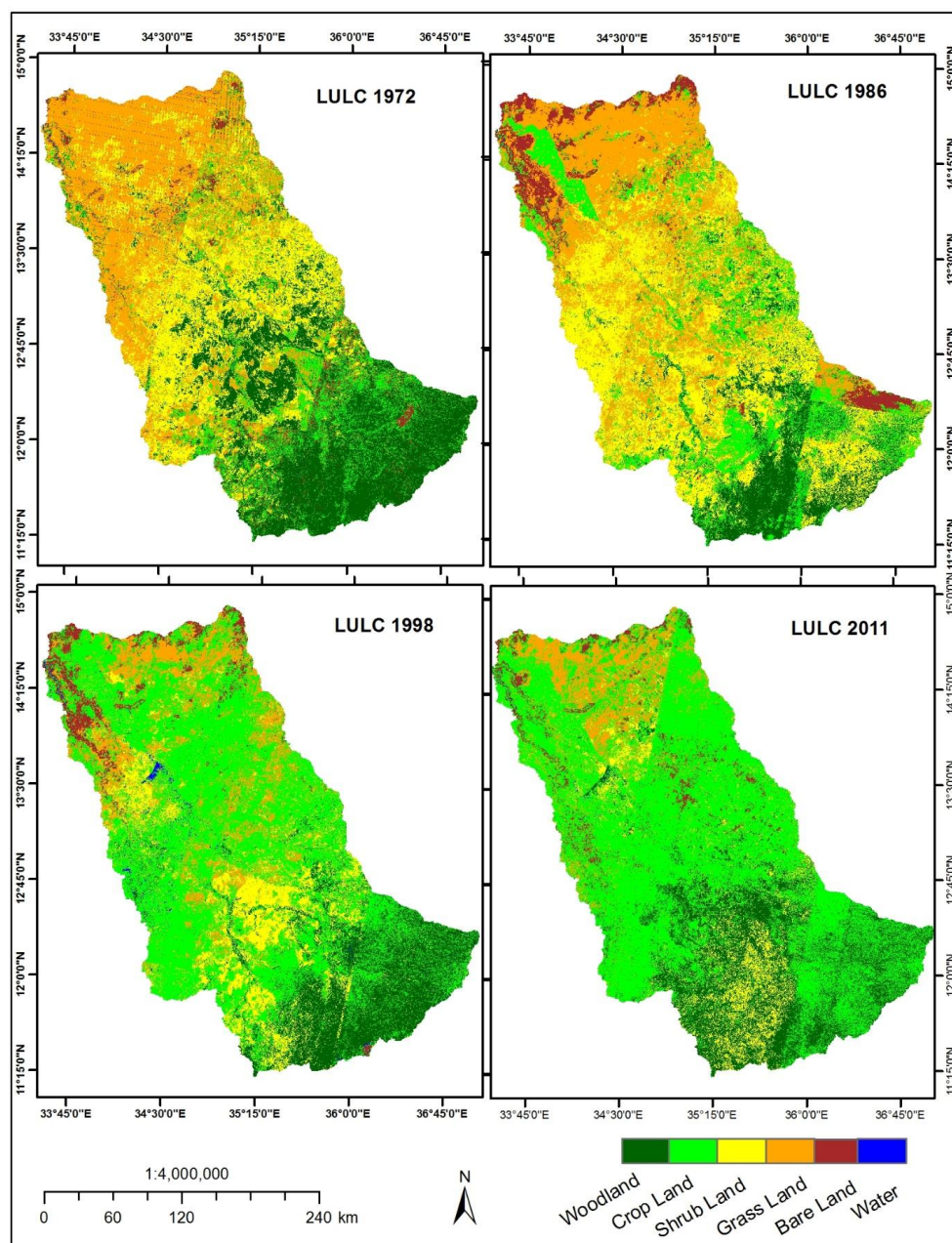
Figure 3. Classified LULC maps of the years 1972, 19986, 1998 and 2011.

5   Table 3 shows the percentages of LULCC classes in Dinder and Rahad basins that occurred in the period 1972 to 1986, 1986 to 1998, and 1998 to 2011. The decrease in the woodland area in 1986 is mainly attributed to the deforestation during the drought time in 1984 and 1985. As a result, the cropland was increased due to the development of new agricultural areas in both irrigated (i.e. Rahad Agricultural Scheme) and rain-fed sectors. The rapid expansion in the mechanized rain-fed

agriculture led to a large increase in cropland during 1998 and 2011. These findings are in agreement with what have been reported by Marcotullio and Onishi (2008), and Biro et.al, (2013) from their similar studies conducted in the Ethiopian highlands and Gedarif region in eastern Sudan.

5   Table 3: Land cover changes (%) in Dinder and Rahad basins that occurred in the period 1972 to 1986, 1986 to 1998, and 1998 to 2011.

Land cover type (%)	Dinder				Rahad			
	1972	1986	1998	2011	1972	1986	1998	2011
Bare area	5	1	0	2	6	5	0	3
Woodland	42	23	27	14	35	14	21	14
Shrubland	23	43	21	36	30	32	13	15
Grassland	16	18	5	1	11	22	9	1
Cropland	14	15	45	47	18	26	55	68

4.1.1   Calibration and validation of the hydrological model results

10   The NSE and R^2 ranged from 0.4 to 0.80 and 0.50 to 0.80, respectively for the daily calibration and validation for the three precipitation products at Al-Gewisi station on the Dinder River and Al-Hawata station on the Rahad River (Fig. 4 and 5). The calibration results indicate that CHIRPS 2.0 is the best products over rugged terrain with complex rainfall patterns in the D&R basins. This result is in agreement with Hessels (2015), who compared and validated 10 open-access and spatially distributed satellite rainfall products over the Nile Basin and found that CHIRPS is the best product to be used in the Nile

15   Basin. The modelling results show that the approach is reasonably good and therefore can be used in predicting runoff at a sub-basin level. Then the model was used to simulate the impact of LULCC on streamflow by running the model using land cover from different periods of time (1972, 1986, 1998 and 2011) and keeping precipitation (CHIRPS), evapotranspiration and other model parameters without change.
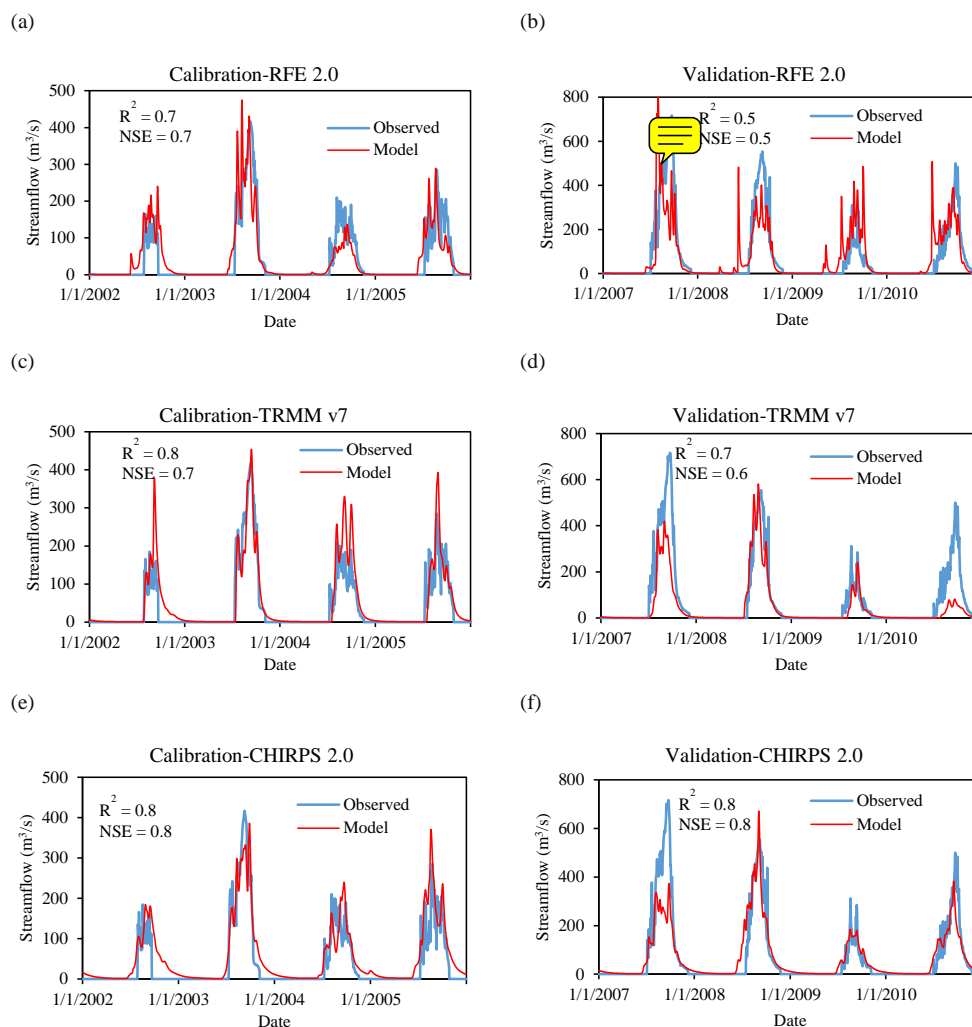
20

25

30

35

Figure 4. Calibration and validation results at Al-Gewisi station on Dinder River (a) and (b) for RFE, (c) and (d) for TRMM and (e) and (f) for CHIRPS.
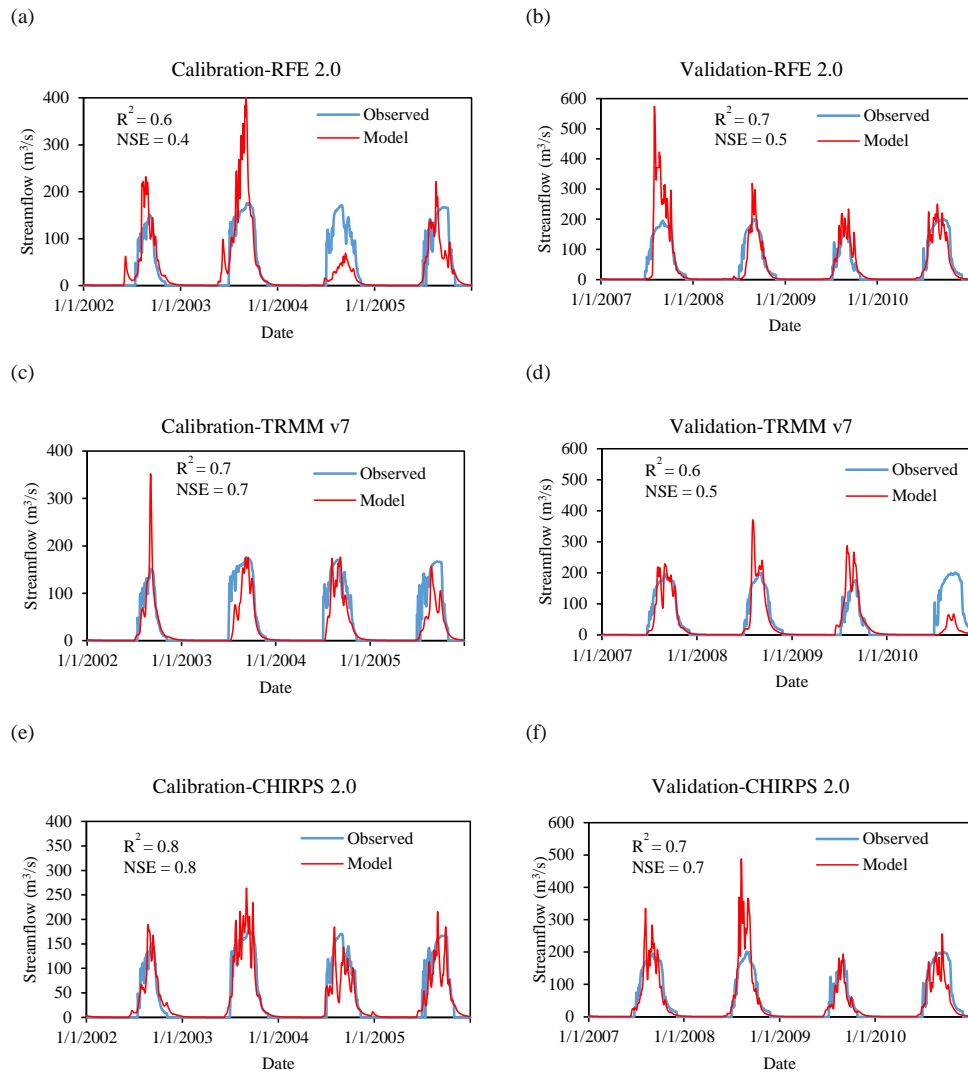
5

10

15

Hydrology and
Earth System
Sciences
Open Access
EGU
Discussions

(a)   (b)

(c)   (d)

(e)   (f)

Figure 5. Calibration and validation results at Al-Hawata station on Rahad River (a) and (b) for RFE, (c) and (d) for TRMM and (e) and (f) for CHIRPS.

4.2   Streamflow response under land cover conversions

5   After the calibration and validation of the WFlow, the model has been run using different land use with fixed model parameters. First with land use from 1972; second with land use from 1986; third with land use from 1998; and fourth with land use from 2011. Then the outputs from the four land use were compared. We note that the rainfall (CHIRPS) and PET for the period 2001-2012 were used with the 1972, 1986, 1998 and 2011 land use to identify hydrological impacts of changes in land cover explicitly.

10   The WFlow result indicates that streamflow is affected by LULCC in both Dinder and Rahad Rivers. The effect of LULCC is much larger in Rahad than in Dinder. In the Rahad basin, the simulated streamflow showed low peak flow with land use of 1972 and high flow with land use of 2011. Woodland and shrubland are dominants in 1972 and occupied 35% and 30% of the

upper catchment area respectively. While cropland is the dominant land cover type in 2011 which occupied 68% .Woodland and shrubland have high porosity and they delayed the release of water to the catchment outlet. Woodland removal implies less infiltration due to a decrease in soil permeability and less interception of rainfall by the tree canopies and thus more runoff and high flow peaks. The daily streamflow of the Dinder and the Rahad as results from different LULC are shown in Fig. 6.

5   Figure 7.a shows the simulated streamflow of the Rahad River as a result from land covers of 1972, 1986, 1998 and 2011. Annual streamflow increased by 75% between 1972 and 1986, but is followed by a decrease of 45% between 1986 and 1998. The increase of streamflow could be a result of a decrease in woodland by 60% from 35% in 1972 to 14% in 1986 associated with an increase in cropland and grassland. Cropland has increased by 44% from 18% in 1972 to 26% in 1986 and grassland has increased by 100% from 11% in 1972 to 22% in 1986. This increase of grassland thus decreases water infiltration due to

10   soil compaction caused by grazing which causes both higher runoff and an increase in annual streamflow magnitude. During the period 1986-1998, cropland and woodland showed a significant increase by 113% and 53%, respectively, while the remaining categories showed declines. During the period 1998-2011, the annual streamflow increased by 65% and corresponds with results on increases in the percentage of bare land, cropland, and shrubland by 754%, 23% and 15%, respectively, while a decrease in woodland and grassland by 37%, and 94%, respectively.

15   Similar to Rahad, the simulated streamflow of the Dinder River showed low peak flow with land use of 1972 and relatively high flow with land use of 2011. Woodland is dominant in 1972 and occupied 42% of the total catchment area. While cropland is the dominant land cover type in 2011 which occupied 47%. Figure 7.b shows the simulated annual streamflow of the Dinder River as a result from land covers of 1972, 1986, 1998 and 2011. Annual streamflow increased by 20% between 1972 and 1986 but is followed by a decrease of 9% between 1986 and 1998. This could be a result of a decrease

20   in woodland by 43% from 42% in 1972 to 23% in 1986 associated with an increase in shrubland, grassland and cropland by 83%, 10% and 6%, respectively. During the period 1986-1998, cropland and woodland increased by 192% and 16%, respectively, while the remaining categories showed declines. Over the period 1998-2011, the annual streamflow increased by 52% and corresponds with findings on increases in the percentage of bare land, cropland, and shrubland by 360%, 4% and 71%, respectively, while a decrease in woodland and grassland by 50%, and 76%, respectively. The decrease in percentage

25   change of bare area over the period 1986-1998, beside the increase in woodland in both the Dinder and the Rahad basins indicate that the environment was recovering from the severe drought of 1984/1985.
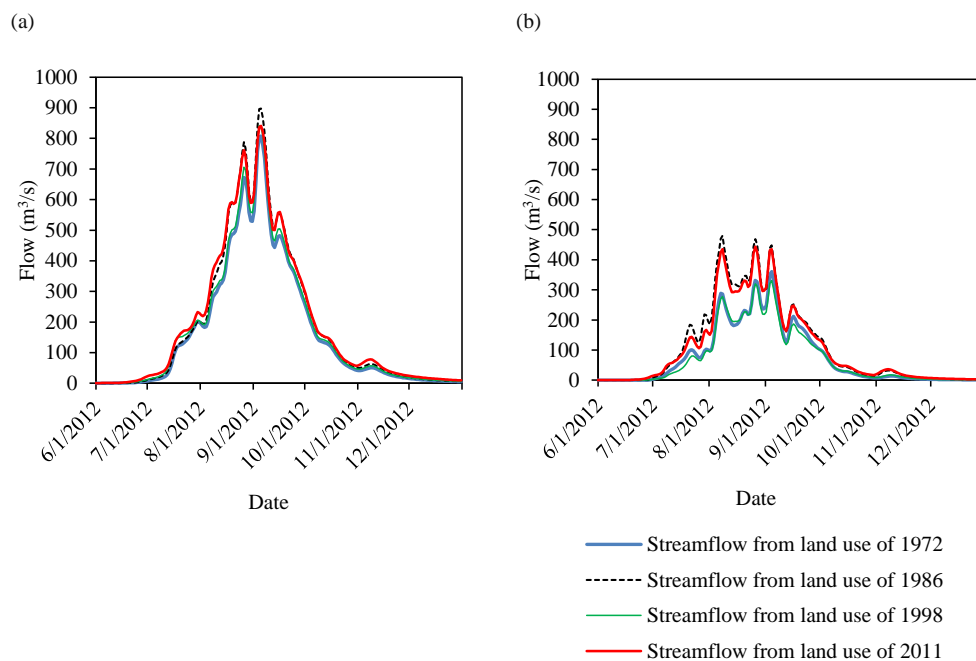
30

Figure 6. Daily streamflow results from the WFlow model at (a) Al-Gewisi station on the Dinder River and (b) Al-Hawata station on the Rahad River based on land use from 1972, 1986, 1998 and 2011 for the year 2012 as an example.
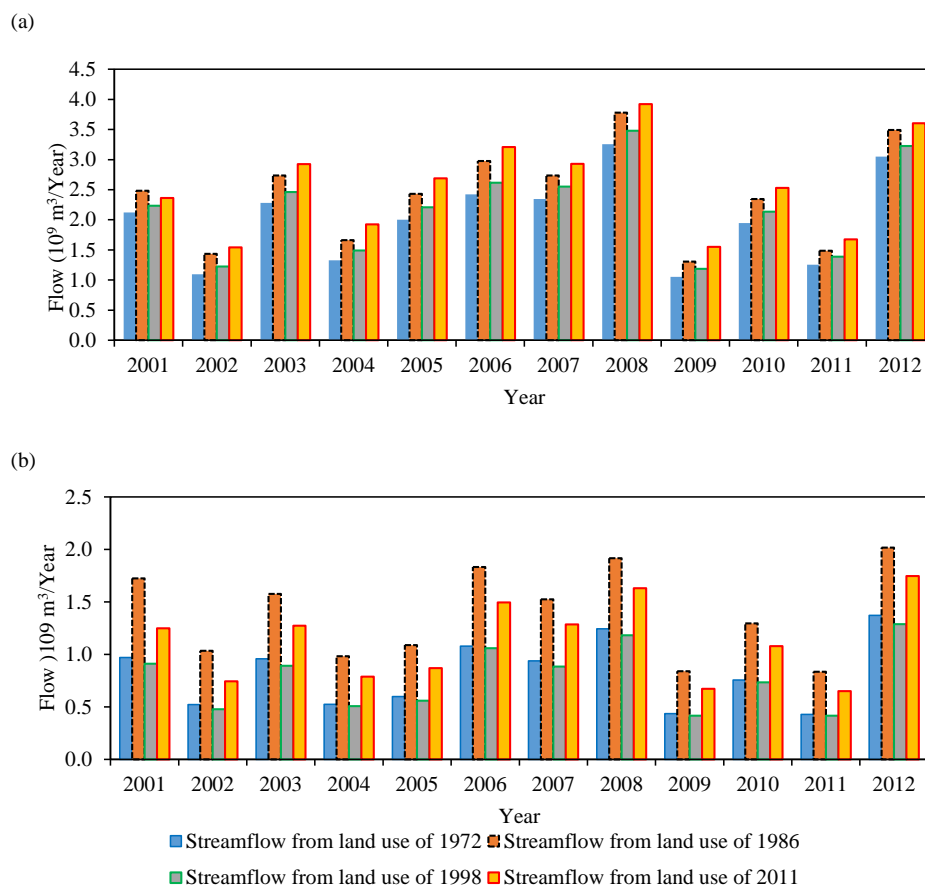
5

10

15

20

(a)

(b)

Figure 7. Annual streamflow results from the WFlow model at (a) Al-Gewisi station on the Dinder River and (b) Al-Hawata station on the Rahad River based on land use from 1972, 1986, 1998 and 2011

5   **4.3**   **Streamflow analysis with IHA**

Since both Dinder and Rahad are seasonal rivers (July-November) and its floodplains including the mayas are mainly depending on floods, the streamflow analysis is focused on the flows during the months of high flows and the indicators describing the hydrological high extremes. The investigated streamflow variables are a subset of the 32 indicators proposed by Richter et al. (1996) under the Range of Variability approach (RVA) that characterizes the natural flow regime of a river

10   into five categories of magnitude, timing, duration, frequency and rate of change. In this section, we analyzed the modelled streamflow as a result from LULC of 1972, 1986, 1998 and 2011.

4.3.1   **Magnitude of monthly flow**

The general pattern of median monthly flow of the Rahad River (Fig. 8a) at Al-Hawata station during 1972-1986 is that the median flow increased in all months of flow (July-November) with an average of 83% per month. In contrast, the median

15   monthly flow decreased in all months during the period 1986-1998 with an average of 45% per month. Similar to the period from 1972-1986, the median monthly flow during 1998-2011 increased by an average of 65% per month.

In comparison to Rahad, the Dinder median monthly flow (Fig. 8b) at Al-Gewisi station during 1972-1986 increased in all

months of flow by an average of 21% per month. In contrast, the median monthly flow decreased in all months during the period 1986-1998 with an average of 6% per month. Likewise, to the period from 1972-1986, the median monthly flow during 1998-2011 increased by an average of 17% per month. Alterations of the monthly flow magnitude, particularly during the months of high flows (August-October) is likely affecting habitat availability on floodplains, which may lead to decrease

5   and/or disappearance of native flora and increase in non-natives flora that might not be suitable for the herbivores wildlife that dwells in the DNP.
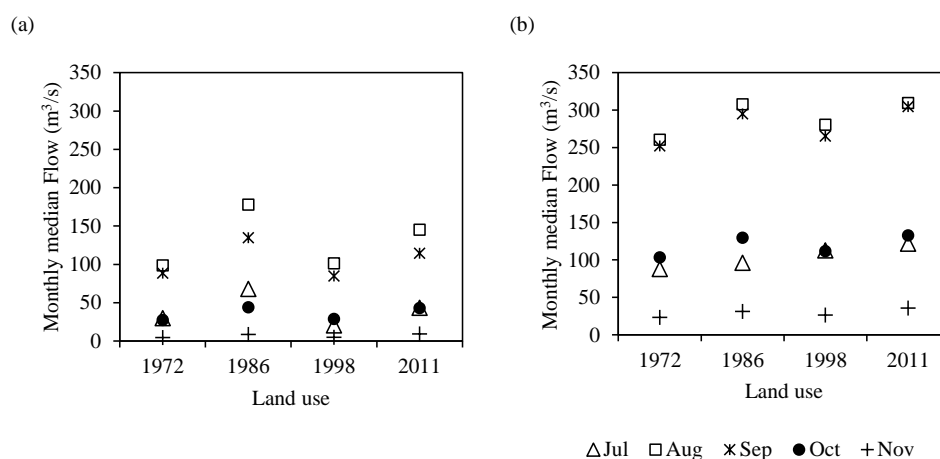
Figure 8. The monthly median flow (a) for Rahad River and (b) for Dinder River

4.3.2   Magnitude of river extreme floods

Extreme floods are important in re-forming both the biological and physical structure of a river and its associated floodplain. Extreme floods are also important in forming key habitats such as oxbow lakes and floodplain wetlands. The pattern of the

15   extreme flow is vital for the filling of wetland mayas of the DNP. Therefore, annual flow maxima of 1, 7, 30 and 90-day have been investigated. The median maxima are presented in Fig. 9. In general, all results have shown that the maxima's are significantly affected by LULCC. In Rahad median flow maxima for 1, 7, 30 and 90-day intervals from the land use of 1986 are 51 %, 56%, 67%, and 68%, respectively higher than the maxima's from the land use of 1972. Likewise, median flow maxima for 1, 7, 30 and 90-day intervals from the land use of 2011 are 32 %, 33%, 36%, and 39%, respectively higher than

20   the maxima's from the land use of 1998. In contrast, median flow maxima for 1, 7, 30 and 90-day intervals from the land use of 1998 are 39 %, 39%, 42%, and 42%, respectively lower than the maxima's from the land use of 1986.

In the Dinder River the effect of LULCC on streamflow is not big as in Rahad River. The median flow maxima for 1, 7, 30 and 90-day intervals from the land use of 1986 are 19 %, 19%, 18%, and 18%, respectively higher than the maxima's from the land use of 1972. Likewise, median flow maxima for 1, 7, 30 and 90-day intervals from the land use of 2011 are

25   14 %, 13%, 14%, and 19% respectively higher than the maxima's from the land use of 1998. In contrast, median flow maxima for 1, 7, 30 and 90-day intervals from the land use of 1998 are 11 %, 11%, 10%, and 10%, respectively lower than the maxima's from the land use of 1986. Peak flows are the critical aspects of the lateral connectivity between the Rahad and the Dinder rivers and its floodplains. Reduction of the magnitude of these high flow peaks during dry years (less than average) may reduce the ecological function of the mayas wetlands areas as breeding, nursery and feeding habitat for wildlife.
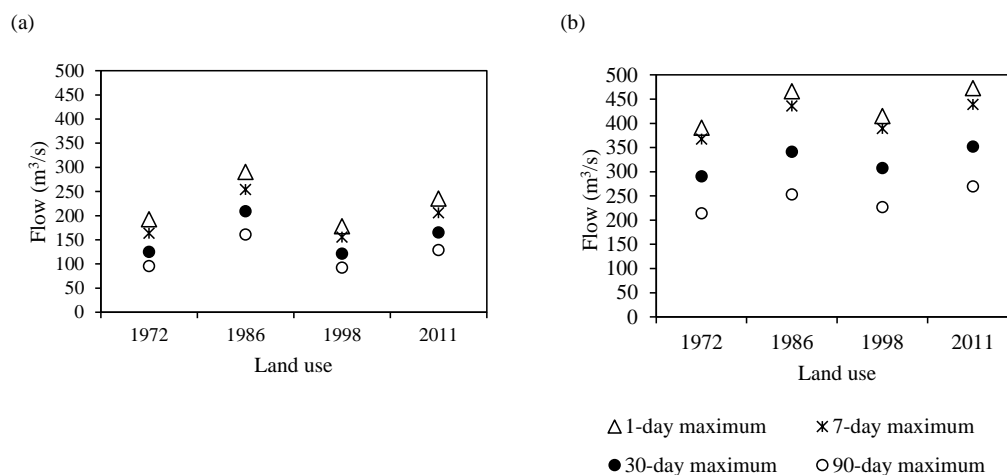
Hydrology and
Earth System
Sciences
Discussions
Open Access

(a)   (b)

△ 1-day maximum   ✳ 7-day maximum
● 30-day maximum   ○ 90-day maximum

Figure 9. Median flow maxima for 1, 7, 30 and 90-day intervals from the land use of 1972, 1986, 1998 and 2011 for (a) Rahad River and (b) Dinder River.

5

4.3.3   Timing of annual extreme floods

Synchronization of annual flood with a variety of riverine and floodplain species life-cycle requirements is of likely high importance given the adaptation of species to their habitat. In Rahad River, date of the annual maxima as results from the land use of 1972, 1986, 1998 and 2011 occurred within the same three weeks (15 August – 02 September, Julian date (JD) 227–

10 245). The annual maxima from the land use of 1986 is 18 days earlier than the annual maxima from land use of 1972. This could be attributed to land cover degradation and deforestation due to the devastating drought of 1984/1985 result in accelerating the runoff response.

In Dinder River, date of the annual maxima are not affected by LULCC and occurred within the same two days (11 September – 12 September, Julian date (JD) 254–255).

15 ### 4.3.4   Rate of change in flow

The rate of change in flow can affect persistence and lifetime for both aquatic and riparian species (Poff et al. 1997), particularly in arid areas where streamflow usually changes rapidly in a very short time. Figure 10 shows the rate of flow-rises and flow-falls for both Rahad and Dinder. The median rate of flow-rises (positive differences between consecutive daily values) in Rahad River has increased by 74% from 2.73 (m^3/s) /day in 1972 to 4.73 (m^3/s) /day in 1986. In 1998 the median rate of flow-

20 rises decreased by 50%, while increasing by 37% in 2011. Similarly, the median rate of flow-falls (negative differences between consecutive daily values) has increased by 88% from 0.12 (m^3/s) /day in 1972 to 0.23 (m^3/s) /day in 1986. In 1998 the median rate of flow-falls decreased by 37%, while increasing by 22% in 2011. Likewise, the median rate of flow-rises and flow-falls in the Dinder River follow the same pattern of the Rahad flow, but no significant changes were observed. This result shows that the fluctuation in rate of change in streamflow is strongly linked to LULCC, especially when analyzing the

25 streamflow as a result from land use after a period of drought (e.g. land use of 1986).

Hydrology and
Earth System
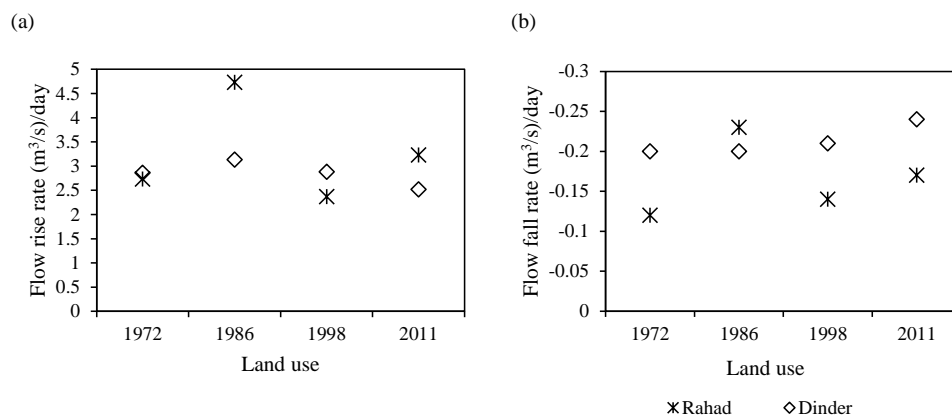Sciences

Open Access

Discussions

EGU

Figure 10. The rate of flow rises (a) and falls (b) as a response to land use of 1972, 1986, 1998 and 2011 for both Rahad and Dinder Rivers (negative sign in the vertical axis indicates downward direction of flow).

5   Conclusion

5   For assessing the changes in land cover, four remote sensing images were used for the years 1972, 1986, 1998 and 2011. The accuracy assessment with supervised land cover classification shows that the classification results are reliable. The land cover changes in the D&R are assessed by image comparison and the results showed that the dominant process is the relatively large decrease of woodland and the large increase of cropland. Results of LULCC detection between 1972 and 2011 indicate a significant decrease of woodland and an increase of cropland. Woodland decreased from 42% to 14% and from 35% to 14%

10   for Dinder and Rahad respectively. Cropland increased from 14% to 47% and from 18% to 68% in Dinder and Rahad respectively. The rate of deforestation is high during the period 1972-1986 and probably is due to the severe drought during 1984/1985, expansion in agricultural activities and increased demand for wood for fuel, construction and other human needs due to the increase in population. On the other hand, increasing in woodland during the period between 1986 and 1998 is probably due to reforestation activities in the basin. Nevertheless, the magnitude of deforestation is still much larger than the

15   reforestation. The cropland expansion over the period 1986 to 1998 is larger than the expansion over the period 1998 to 2011, suggests that most of the areas that are suitable for cultivation have most likely been occupied, or the land tenure regulations have controlled the expansion of cultivation by local communities.

         The results of the hydrological model indicate that streamflow is affected by LULCC in both the Dinder and the Rahad Rivers. The effect of LULCC on streamflow is significant during 1986 and 2011 particularly in Rahad River. This could

20   be attributed to the severe drought during 1984/1985 and the large expansion in cropland in the Rahad catchment to 68% of the total area.

         The IHA analysis indicated that the flow of the Dinder and the Rahad Rivers was associated with significant upward and downward alterations in magnitude, timing and rate of change of river flows, as a result of LULCC. These alterations in the streamflow characteristics are likely to have significant effects on a range of species that depend on the seasonal patterns of flow. Therefore, alterations in the magnitude of the annual floods that decrease the water flowing to the mayas may reduce

25

the production of native river-floodplain fauna and flora, and migration of animals that may be connected to mayas inundation.

Competing interests: The third author is a member of the editorial board of the journal.

30

Hydrology and
Earth System
Sciences
Discussions

Open Access

EGU

5

References

Al Fugara, A. M., Pradhan, B. and Mohamed, T. A.: Improvement of land-use classification using object-oriented and fuzzy logic approach, Appl. Geomat, 1, 111-120, 2009.

Bates, P. and De Roo, A.: A simple raster-based model for flood inundation simulation, J. Hydrol, 236, 54-77, 2000.

Bewket, W. and Sterk, G.: Dynamics in land cover and its effect on stream flow in the Chemoga watershed, Blue Nile basin, Ethiopia, Hydrol. processes, 19, 445-458, 2005.

Bewket, W. and Teferi, E.: Assessment of soil erosion hazard and prioritization for treatment at the watershed level: Case study in the Chemoga watershed, Blue Nile basin, Ethiopia, Land Degrad. Dev, 20, 609-622, 2009.

Biro, K., Pradhan, B., Buchroithner, M. and Makeschin, F.: Land use/land cover change analysis and its impact on soil properties in the northern part of Gadarif region, Sudan, Land Degrad. Dev, 24, 90-102, 2013.

Block, P. and Rajagopalan, B.: Interannual variability and ensemble forecast of Upper Blue Nile Basin Kiremt season precipitation, J. Hydrometeorol, 8, 327-343, 2006.

DeFries, R. and Bounoua, L.: Consequences of land use change for ecosystem services: A future unlike the past, GeoJournal, 61, 345-351, 2004.

DeFries, R. and Eshleman, K.: Land‐use change and hydrologic processes: a major focus for the future, Hydrol. processes, 18, 2183-2186, 2004.

Deursen van, W. P. A.: Geographical Information Systems and Dynamic Models. Ph.d., Utrecht University, NGS Publication 190, 198 pp., URL, http://www.carthago.nl, 1995.

Ellis, E. A., Baerenklau, K. A., Marcos-Martínez, R. and Chávez, E.: Land use/land cover change dynamics and drivers in a low-grade marginal coffee growing region of Veracruz, Mexico, Agrofor. Syst, 80, 61-84, 2010.

Funk, C. C., Peterson, P. J., Landsfeld, M. F., Pedreros, D. H., Verdin, J. P., Rowland, J. D., Romero, B. E., Husak, G. J., Michaelsen, J. C. and Verdin, A. P.: A quasi-global precipitation time series for drought monitoring, US Geological Survey Data Series, 832, 2014.

Gash, J.: An analytical model of rainfall interception by forests, Q. J. R. Meteorolog. Soc, 105(443), 43-55, 1979.

Gash, J. H. C., Lloyd, C. R., and Lachaud, G.: Estimating sparse forest rainfall interceptionwith an analytical model, J. Hydrol, 170:79–86, 1995.

Gumindoga, W., Rientjes, T. H. M., Haile, A. T. and Dube, T.: Predicting streamflow for land cover changes in the Upper Gilgel Abay River Basin, Ethiopia: A TOPMODEL based approach, Phys. Chem. Earth., Parts A/B/C, 76–78, 3-15, doi:http://dx.doi.org/10.1016/j.pce.2014.11.012, 2014.

Hansen, A., DeFries, R. and Turner, W.: Land Use Change and Biodiversity: A Synthesis of Rates and Consequences during the Period of Satellite Imagery in: Land Change Science: Observing, Monitoring, and Understanding Trajectories of Change on the Earth's Surface Springer Verlag, New York, NY., 277-299, 2004.

Hassaballah, K., Mohamed, Y. A. and Uhlenbrook, S.: The Mayas wetlands of the Dinder and Rahad: tributaries of the Blue Nile Basin (Sudan), in: The Wetland Book: II: Distribution, Description and Conservation, (eds C. Max Finlayson, G. Randy Milton, R. Crawford Prentice, and Nick C. Davidson) Springer Netherlands, 1-13, 2016.

Hemmavanh, C., Ye, Y. and Yoshida, A.: Forest land use change at Trans-Boundary Laos-China Biodiversity Conservation Area, J. Geogr. Sci., 20, 889-898, doi:10.1007/s11442-010-0818-1, 2010.

Hessels, T. M.: Comparison and Validation of Several Open Access Remotely Sensed Rainfall Products for the Nile Basin, TU Delft, Delft University of Technology, 2015.

Huffman, G. J. and Bolvin, D. T.: TRMM and other data precipitation data set documentation, NASA, Greenbelt, USA, 1-40, 2013.

Hurni, H., Tato, K. and Zeleke, G.: The implications of changes in population, land use, and land management for surface runoff in the upper Nile basin area of Ethiopia, Mt. Res. Dev, 25, 147-154, 2005.

Hurst, H., Black, R. and Simaika, Y.: The Nile Basin, vol. IX. The hydrology of the Blue Nile and Atbara and the Main Nile to Aswan, with reference to some Projects, Ministry of Public Works, Physical Department, Cairo, Egypt, 1959.

Jensen, J. R.: Digital change detection. Introductory digital image processing: A remote sensing perspective, Prentice Hall, Upper Saddle River, NY, 525 pp., 2005.

Kamusoko, C. and Aniya, M.: Hybrid classification of Landsat data and GIS for land use/cover change analysis of the Bindura district, Zimbabwe, Int. J. Remote Sens, 30, 97-115, 2009.

Karssenberg, D.: The value of environmental modelling languages for building distributed hydrological models, Hydrol. Processes, 16, 2751-2766, 2002.

Köhler, L., Mulligan, M., Schellekens, J., Schmid, S. and Tobón, C.: Final Technical Report DFID-FRP Project no. R7991 Hydrological impacts of converting tropical montane cloud forest to pasture, with initial reference to northern Costa Rica, 2006.

Marcotullio, P. J. and Onishi, T.: The impact of urbanization on soils, in: Land use and soil resources, Springer, 201-250, 2008.

Metzger, M., Rounsevell, M., Acosta-Michlik, L., Leemans, R. and Schröter, D.: The vulnerability of ecosystem services to land use change, Agric. Ecosyst. Environ, 114, 69-85, 2006.

Mundia, C. and Aniya, M.: Dynamics of landuse/cover changes and degradation of Nairobi City, Kenya, Land Degrad. Dev, 17, 97-108, 2006.

Nash, J. E. and Sutcliffe, J. V.: River flow forecasting through conceptual models part I—A discussion of principles, J. Hydrol, 10, 282-290, 1970.

Pettitt, A.: A non-parametric approach to the change-point problem, Applied statistics, 126-135, 1979.

Poff, N. L., Allan, J. D., Bain, M. B., Karr, J. R., Prestegaard, K. L., Richter, B. D., Sparks, R. E. and Stromberg, J. C.: The natural flow regime, BioScience, 769-784, 1997.

Polasky, S., Nelson, E., Pennington, D. and Johnson, K.: The Impact of Land-Use Change on Ecosystem Services, Biodiversity and Returns to Landowners: A Case Study in the State of Minnesota, Environ Resource Econ, 48, 219-242, doi:10.1007/s10640-010-9407-0, 2011.

Pradhan, B. and Suleiman, Z.: Landcover mapping and spectral analysis using multi-sensor satellite data fusion techniques: case study in Tioman Island, Malaysia, J. Geomat, 3, 71-78, 2009.

Richards, J., Xiuping, J., Gessner, W. and Ricken, D.: Remote sensing digital image analysis, 4th edition-Springer-Verlag, Berlin Heidelberg, ISBN: 13 978-973-540-25128-25126. pp.25194 – 25199., 2006.

Richter, B. D., Baumgartner, J. V., Powell, J. and Braun, D. P.: A method for assessing hydrologic alteration within ecosystems, Conserv. biol, 10, 1163-1174, 1996.

Schellekens, J.: WFlow , a flexible hydrological model, 2011.

Shahin, M.: Hydrology of the Nile basin. Series title Vol. 21 Elsevier Science and Technology, 1985.

Teferi, E., Bewket, W., Uhlenbrook, S. and Wenninger, J.: Understanding recent land use and land cover dynamics in the source region of the Upper Blue Nile, Ethiopia: Spatially explicit statistical modeling of systematic transitions, Agric. Ecosyst. Environ, 165, 98-117, doi:http://dx.doi.org/10.1016/j.agee.2012.11.007, 2013.

Turner, B. L., Matson, P. A., McCarthy, J. J., Corell, R. W., Christensen, L., Eckley, N., Hovelsrud-Broda, G. K., Kasperson, J. X., Kasperson, R. E. and Luers, A.: Illustrating the coupled human–environment system for vulnerability analysis: three case studies, Proceedings of the National Academy of Sciences, 100, 8080-8085, 2003.

5   Turner, B. L., Lambin, E. F. and Reenberg, A.: The emergence of land change science for global environmental change and sustainability, Proceedings of the National Academy of Sciences, 104, 20666-20671, 2007.

Uhlenbrook, S.: Biofuel and water cycle dynamics: what are the related challenges for hydrological processes research?, Hydrological processes, 21, 3647-3650, 2007.

Uhlenbrook, S., Roser, S. and Tilch, N.: Hydrological process representation at the meso-scale: the potential of a distributed, conceptual catchment model, J. Hydrol, 291, 278-296, 2004.

10   Vertessy, R. A. and Elsenbeer, H.: Distributed modeling of storm flow generation in an Amazonian rain forest catchment: Effects of model parameterization, Water Resour. Res, 35, 2173-2187, 1999.

Wesselung, C. G., Karssenberg, D. J., Burrough, P. A., and Deursen, W.: Integrating dynamic environmental models in GIS: the development of a Dynamic Modelling language. Transactions in GIS, 1(1), 40-48, 1996

Yuan, F., Bauer, M. E., Heinert, N. J. and Holden, G. R.: Multi‐level land cover mapping of the Twin Cities (Minnesota) metropolitan area with multi‐seasonal Landsat TM/ETM+ data, Geocarto. Int, 20, 5-13, 2005.

15

Zeleke, G. and Hurni, H.: Implications of land use and land cover dynamics for mountain resource degradation in the northwestern Ethiopian highlands, Mt. Res. Dev, 21, 184-191, 2001.

20